Metallomics

Accepted Manuscript

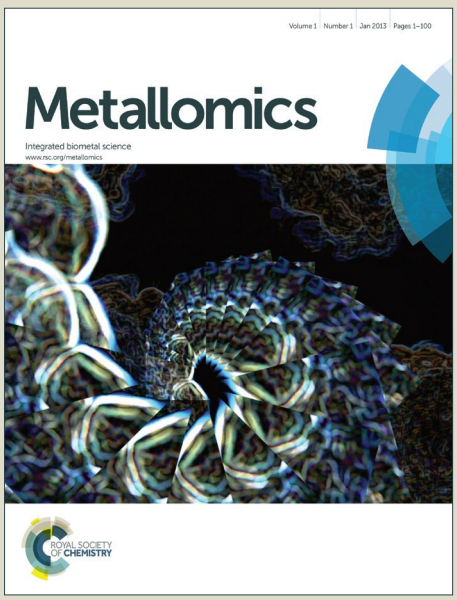

ROYAL SOCIETY OF CHEMISTRY

www.rsc.org/metallomics

Copper, differently from zinc, affects bradykinin conformation, oligomerization state and activity

Irina Naletova,[1,2] Vincenzo G. Nicoletti,[1,2*] Danilo Milardi,[3] Adriana Pietropaolo,[4] Giuseppe Grasso[5*]

1 Dipartimento di Scienze Biomediche e Biotecnologiche "BIOMETEC", Università degli Studi di Catania, Via S. Sofia 64, 95125 Catania, Italy.

2 Consorzio Interuniversitario di Ricerca in Chimica dei Metalli nei Sistemi Biologici (C.I.R.C.M.S.B.), Piazza Umberto I, 1 – 70121 Bari, Italy.

3 Istituto di Biostrutture e Bioimmagini, Via Paolo Gaifami 18, 95126 Catania.

4 Dipartimento di Scienze della Salute, Università di Catanzaro, Campus Universitario, Viale Europa, 88100 Catanzaro, Italy.

5 Dipartimento di Scienze Chimiche, Università di Catania, Viale Andrea Doria 6, 95125, Catania, Italy.

*Correspondence to:

Giuseppe Grasso, Dipartimento di Scienze Chimiche, Università degli Studi di Catania, Viale Andrea Doria 6, 95125, Catania, Italy. e-mail: grassog@unict.it

Vincenzo G. Nicoletti, Dipartimento di Scienze Biomediche e Biotecnologiche "BIOMETEC", Università degli Studi di Catania, via S. Sofia 64, 95125 Catania, Italy. Email: nicovigi@unict.it

Abstract

The sole role of bradykinin (BK) as an inflammatory mediator is controversial, as recent data also support an anti-inflammatory role for BK in Alzheimer's Disease (AD). The involvement of two different receptors (B_1R and B_2R) could be a key to understand this issue. However, although copper and zinc dyshomeostasis have been demonstrated to be largely involved with the development of AD, a detailed study of the interaction of BK with these two metal ions has never been addressed. In this work, we have applied mass spectrometry, circular dichroism as well as computational methods in order to assess if copper and zinc have the ability to modulate BK conformation and oligomerization. In addition, we have correlated the chemical data with the metals effect on the BK activity analyzed in cell cultures by biochemical procedures.

The biochemical analyses of BK effects on monocyte/macrophage cell culture (THP-1 Cell Line human) in line with the metals effect on BK conformation, showed that the presence of copper can affect the signaling cascade mediated by the BK receptors. The results obtained open to further role of metal ions, particularly copper, in the development and outcome of neuroinflammatory diseases. The possible implications in AD are discussed.

Key Words

Bradykinin, copper, zinc, oligomerization, Alzheimer's disease, inflammation.

Introduction

Bradykinin (BK) is a peptide containing nine amino acidic residues and is involved in several different biological activities, being a potent inflammatory mediator that is produced in both brain and peripheral cells under pathophysiological conditions such as trauma, stroke, ischemia, and asthma. BK is able to decrease blood pressure, increase vascular permeability and promote the classical symptoms of inflammation such as vasodilation, hyperthermia, edema, and pain.[1] Levels of BK in humans can vary considerably depending on localization (on average, in plasma [BK] ≅ $4*10^{-10}$ M, in the brain [BK] ≅ $1*10^{-9}$ M)[2] and on specific conditions (BK concentrations *in vivo* range from 60 pM to ≥100 nM in humans).[3] It is important to note that we cannot really know the concentration of BK at the cell surface in the vicinity of the receptor and theoretically this concentration could be micromolar in that membrane domain to evoke receptor activation. In pathological conditions, a rise in the level of BK in the respiratory system causes acute respiratory distress syndrome, dry cough, inflammation, and apoptosis via release of proinflammatory mediators such as cytokines and chemokines, while growing evidence also suggests a role for BK and its receptors in Alzheimer's disease (AD).[4] For example, a significant increase in densities of kinin B1 and B2 receptors in animals submitted to Aβ infusion was observed in brain regions related to cognitive behavior, suggesting the involvement of the kallikrein-kinin system in AD *in vivo*.[5] Although BK is well recognized as a potent mediator of inflammation,[6] a growing set of evidence suggests an anti-inflammatory role for BK in brain tissues.[7] Indeed, BK applied to neurons can exert inflammatory effects, whereas in glial cells, BK can have a potential protective role for neurons by inhibiting proinflammatory cytokines.[8] Interestingly, an increase of BK release in brain and cerebrospinal fluid (CSF) was found in rats chronically infused with Aβ.[9] However, only a BK degradation product (Arg-Pro-Pro) was found in the brain, indicating the participation of proteases other than angiotensin converting enzyme (ACE) in BK degradation.[10] Moreover, this result indicates that BK degradation products have also to be considered in order to fully understand the

biomolecular role of BK, as generally peptide fragments derived from a precursor protein (cryptides) could have biological roles that are different from the full-length protein.[11]

From these data it is evident that the exact role of BK and/or BK cryptides in AD is not very clear and further studies targeting the potential interactions of BK with other recognized actors of AD are needed. Particularly, transition metal ions such as copper and zinc have been reported to play an important role in AD. Moreover, metal ion levels as well as metal-mediated oxidative damage to neuronal cells, which generally precedes Aβ deposition, have been reported to increase with normal aging.[12] These metals accumulate within the plaque deposits and reach concentrations up to 300 μM.[13] Copper dishomeostasis has been correlated to many pathological states, and a wide range of possible molecular mechanisms and cellular targets have been claimed to be linked to pathological conditions challenged by bad management of copper levels or subcellular distribution. In addition, copper availability/redistribution is known to be responsible of various consequences in the progression of AD (as well as other neurodegenerative diseases), ranging from Aβ conformational changes and prooxidant reactions to alteration of APP maturation. Indeed, using chelators like clioquinol or PBT2 it has been also proved that observed beneficial effects can be due to prevention of extracellular Aβ-metal interactions and redistribution of Cu into cells (Prana Biotechnology Ltd). Moreover, these compounds promote cellular copper uptake, and up-regulation of cell signaling cascade involving a number of molecules with known neuroprotective activity.[14--16] For these reasons, the ‘‘metal hypothesis of AD’’ has been consequently proposed, according to which the abnormal interaction between Aβ and metal ions has to be considered as one of the major culprits for the development of AD.[17] However, if a dyshomeostasis of metal ions occurs in AD, the effect of altered metal ions concentrations and/or redistribution on biomolecules other than Aβ has to be taken into account to give further insights on the mechanisms at the base of AD. For this reason the interactions of copper and zinc with proteins such as ubiquitin,[18-20] BDNF[21] and proteases[22] capable to degrade Aβ have been recently studied by our group.

In the literature, some studies focus on the interaction of BK with metal ions.[23-26] However, the main aim of these studies was related to the design of new artificial catalysts and ACE inhibitors,[23] or the elucidation of gas phase interactions for unveiling the intrinsic preference of each metal ion for particular coordination geometries and ligand types.[24] To the best of our knowledge, none of these studies focus on the role of copper and zinc in BK conformation and oligomerization and how these two metal ions affect BK stability and proneness to degradation. We think that these issues have to be addressed to better define the role of BK and metal ions in AD and, more generally, to ascertain if the interaction of BK with metal ions can have an effect on BK functions. For these reasons, here we have applied mass spectrometry (MS), circular dichroism (CD) as well as computational methods in order to assess if copper and zinc have the ability to modulate BK conformation and oligomerization or have an effect on its stability and proneness to degradation by insulin-degrading enzyme (IDE).[27] Moreover, The biochemical analyses of BK effects on monocyte/macrophage cell culture (THP-1 Cell Line human) in line with the metals effect on BK conformation, showed that the presence of copper can affect the signaling cascade mediated by the BK receptors.

Experimental

Materials and methods

IDE, wild type recombinant, was purchased from GIOTTO Biotech srl. BK and all the other reactants were purchased from SIGMA-ALDRICH.

The enzymatic digestions of BK by IDE were carried out as follows. The peptide at various concentrations was incubated with IDE (8ng/μl) in 10 mM MOPS (pH 7.4) at 37°C, in the presence or absence of the metal ion (copper(II) or zinc(II)) for 60 min. In order to stop the enzymatic reaction, a 10% solution in trifluoroacetic acid (TFA) was added to the different aliquots in order to achieve a final concentration of TFA of 0.2%. Sample solutions were purified by ZIPTIPC18 and

after dilution with 50 µl of water and 50 µl of Methanol were injected into the MS ion source at a flow-rate of 5 µl/min, using nitrogen as drying gas.

Computational analysis

The BK peptide underwent 10 ns of parallel tempering (PT) simulations in explicit solvent, after have been equilibrated through 2 ns of MD in explicit solvent. GROMACS 4.5.6 package[28] was used. The overall charge of the system was neutralized by adding 2 chloride ions. Periodic boundary conditions were applied. The AMBER99SB[29] force field was used for the biomolecules and counter ions, and the TIP3P[30] force field was used for water molecules. Electrostatic interactions were calculated using the Particle Mesh Ewald method.[31] A cutoff (0.9 nm) was used for the Lennard-Jones interactions. The time-step was set to 2 fs. All bond lengths were constrained to their equilibrium values using the SHAKE[32] algorithm for water and the LINCS[33] algorithm for the peptide. We simulated 64 replicas distributed in the temperature range 300-400 K following a geometric progression. All replicas were simulated in NVT ensemble using a stochastic thermostat[34] with a coupling time of 0.1 ps. A thermostat that yields the correct energy fluctuations of the canonical ensemble is crucial in parallel tempering simulations.[35] Exchanges were attempted every 0.1 ps. The method of Daura and Van Gunsteren[36] was used in post-processing phase to cluster the resulting trajectories, with a cutoff of 3 Å calculated on the backbone atoms as implemented in the clustering utility provided in the GROMACS package.[28]

To the former clusters were coordinated to Zn^{2+} and Cu^{2+} in a 1:1 and 2:1 BK:metal stoichiometric ratio. The coordination geometries were optimized at the HF level of theory within the 6-31G** basis sets through the Gaussian 09 revision D.01 package[37] with a root mean square displacement of 10-3 Å. ECD spectra were calculated using the DICHROCALC platform.[38]

Mass Spectrometry

ESI-MS experiments were performed by using a Finnigan LCQ DECA XP PLUS ion trap spectrometer operating in the positive ion mode and equipped with an orthogonal ESI source (Thermo Electron Corporation, USA). The mass spectrometer operated with a capillary voltage of 46 V and capillary temperature of 250°C, while the spray voltage was 4.3 kV. In the presence of Cu^{2+}, the BK-metal ion complex is very sensitive to the ionization potentials, so that, if a high potential (≥1.5 kV) is used, the copper(II) is reduced to copper(I), a behaviour already observed for other copper complexes (see figure 1S).[39]

Circular Dichroism spectroscopy

Far-UV CD spectra of BK were recorded with a Jasco J-810 spectropolarimeter equipped with a Peltier thermally controlled cuvette holder (JASCO PTC- 348). BK concentrations used in CD experiments were in the range of 35 – 100 μM. CD spectra were recorded using a 0.5-cm path length quartz cuvette, from 260 – 190 nm, at 0.1 nm data pitch, 50 nm/min, with a response time of 2 s. All spectra, corresponding to an average of 10 scans, were base-line-corrected by subtracting the signal of the buffer form the CD of the sample. CD curves were recorded in pure water and the pH was adjusted to neutrality by adding NaOH or H_2SO_4. CD spectra are expressed as the mean residue molar ellipticity[40] [θ] expressed in deg cm^2 $dmol^{-1}$:

$$[\theta] = \frac{CD \times 100 \times M}{C \times l \times n} \qquad (1)$$

where CD is the ellipticity in degrees, l is the optical path in cm, M is the molecular weight, n is the number of residues and C is the concentration in mg/ml.

Cell cultures

The human monocytic leukemia cell line THP-1 was grown in RPMI 1640 culture medium (Lonza, Switzerland) supplemented with 10% of fetal bovine serum (FBS; Invitrogen, UK.) and 1% of

penicillin/streptomycin(P/S) (Lonza, Switzerland) at 37 °C in 5% CO_2 in a humidified incubator. LPS (E. coli 0111:B4) was purchased from Sigma.

Macrophage differentiation and stimulation

The mature macrophage-like state was induced by treating THP-1monocytesfor 1 week with 100 ng ml−1phorbol 12-myristate 13-acetate (PMA; Sigma Chemical) in 35 mm cell culture plates (NUNC, Denmark) with 3 ml cell suspension in each well. It has been demonstrated that this differentiation method of THP-1 cells resulted in the expression of macrophage specific surface markers CD11b and CD36 and also phagocytic activity.[41] Differentiated, plastic-adherent cells were washed with RPMI 1640 medium without PMA but containing 2% FBS and 1% P/S. THP-1 monocytes (undifferentiated cells) and THP-1macrophages (differentiated cells) were treated with BK, BK preincubated for 1 hour with copper or zinc (ratio BK:metal=1:2) or with 0.5μg/ml LPS. RPMI 1640 medium containing 2% FBS and 1% P/S was used as a control. Both types of cells were harvested at two different time points 15 min and 20h to investigate phosphorylation and inflammatory pathways. The experiments were performed using 3-4 independent cell culture preparations cells.

MTT Assay

Cell viability of undifferentiated THP-1 (monocytes) was defined as the reduction in MTT [3-(4,5-dimethylthiazol-2-yl)-2,5-diphenyltetrazolium bromide] (Sigma-Aldrich). Living, metabolically active cells reduce the soluble yellow tetrazolium salt MTT, yielding dark blue water-insoluble formazan crystals. MTT was dissolved at a concentration of 5 mg/mL in phosphate-buffered saline (PBS) and RPMI 1640 medium with 1% P/S. Cells were seeded in 24-well plates, and cultured for 24h in 1ml of culture medium containing range of concentrations of tested chemicals. Briefly, whole cell suspension was taken from each well and centrifuged 5 min at 600 g. Supernatant was eliminated, and the pellet was incubated for 1,5 hr in 300 μL of MTT solution per well. This

solution was then replaced with 300 µL of DMSO (Sigma-Aldrich) per well and incubated for 15min at 37°C to dissolve the crystals. Finally, absorbance at 569 nm was measured by a microplate reader spectrophotometer (Multiskan Ascent).

Western blot analysis

After treatment, cells were harvested with RIPA buffer (50mM TRIS-HCl, pH 8,0, 150mM NaCl, 0,5mM EDTA, 1% Triton X-100, 0,5mM EGTA, 1% NP40) containing 2mM PMSF (phenylmethylsulfonylfluoride), inhibitor of proteases (Sigma). Cell lysates were incubated for 30 min and centrifuged at 14000 g for 10 min. Protein concentrations were measured by Bradford method using BSA as standard curve. Equal amounts of protein were separated by 12 % SDS-PAGE and transferred to nitrocellulose membrane (Sigma-Aldrich). The transfers were blocked with blocking buffer (5% BSA in TBST) at room temperature for 1 h, incubated with primary antibodies overnight at 4^{o}C, 1h with horseradish peroxidase-conjugated secondary antibodies. The antibody against IL-1beta (code: ab2105, 1:1,000 dilution) and GAPDH (code: ab8245, 1:2,000 dilution) were purchased from Abcam. The antibody against pErk1/2 (code: 9106, 1:1,000) and β-Actin (code: 4970, 1:2,000 dilution) were from Cell Signaling Technologies, Inc. Goat anti-mouse and anti-rabbit IgG secondary antibody horseradish peroxidase-conjugated (AP181P and AP307P, 1:3,000 dilution) were purchased from Merck Millipore. Detection was conducted using enhanced Super Signal West Pico Chemiluminescent Substrate (Thermo Scientific). Imaging and densitometric analyses were performed by ChemiDoc Imaging System (Bio-Rad).

Results

Mass Spectrometry

The amino acid sequence of BK is Arg-Pro-Pro-Gly-Phe-Ser-Pro-Phe-Arg while its empirical formula is $C_{50}H_{73}N_{15}O_{11}$. BK is easily ionized and detected by ESI-MS as multi-charged molecular

peaks (see figure 2Sa and Table 1 for the assignment). ESI-MS has been widely applied to monitor oligomer formation in solution, as long as experimental parameters are controlled.[42] Here, increasing BK concentration causes the appearance of some other peaks at higher *m/z* values that have been tentatively assigned to BK dimers and trimers and to other molecular species obtained adding Arg or Arg fragments to BK monomers (figure 2Sb, figure 3Sb and Table 1). Unfortunately, the assignment reported in Table 1 could not be verified by MS^2 experiments due to the intrinsic complexity of the molecular species detected. However, it is clear that the formation of more complex species is directly proportional to the BK concentration in solution (figure 3S). The formation of Arg dimers as well as BK dimers in the gas phase is well known and it has been attributed to a salt-bridge ion–zwitterionic structure that stabilizes the dimer, $C(NH_2)_2^+$-$NHCH_2$-CH_2-CH_2-$CH(NH_2)$-COO^--$C(NH_2)_2^+$-NH-CH_2-CH_2-CH_2-$CH(NH_2)$-COOH.[43] Here, the oligomeric BK species reported in Table 1 are detected only for BK solutions with a concentration > 1μM and their detection is directly proportional to the BK concentration used, strongly indicating their presence in the solution phase. Interestingly, increasing the concentration of BK also induces a shift in the multi-charged envelope detected by ESI-MS, that is shifted towards more charged ions. As the pH was kept constant (6.5), this indicates a lowering in the pK of the protonable groups of the molecule, due to a concentration dependent change of the electrostatic interactions of BK solutions. To investigate if metal ions are able to alter the above suggested concentration dependent oligomerization of BK, we have acquired mass spectra in the *m/z* range of, respectively, 200-1600 (figure 4S) and 2000-4000 for BK solutions containing $ZnSO_4$ (figure 5S) or $CuSO_4$ (figure 6S) as indicated. It is not possible to draw any quantitative conclusions based on the absolute intensity of the peaks because different species might ionize differently. However, it is acceptable to assume that copper(II) and zinc(II) BK complexes ionize in a similar manner in the gas phase and that their relative intensities to apo-BK could give a semi-quantitative estimation of the relative concentrations of the species in solution.[44] Based on these two assumptions, figure 4S would indicate that, at the same experimental conditions, the BK-Cu^{2+} complex is more abundant than the

BK-Zn^{2+} complex, the peaks at *m/z* 374.5, 561.2, 1121.4 and 1219.3 (see Table 1 for the assignment) having a higher relative intensities in comparison to the Zn analogous ones. This result is in line with the complex stabilities dictated by the Irving-Williams series, according to which copper(II) complexes are thermodynamically more stable than zinc(II) ones.[45] The absence of peaks in the *m/z* 2000-4000 range might induce to think that precipitation of the peptide is occurring upon copper addition. However, in figure 7S the mass spectrum detected for BK 30 μM and $CuSO_4$ 300 μM in the *m/z* 250-1500 range is also reported and while an intense signal is detected for both apo-BK and BK-copper species, the relative intensities of these species show that the formation of the copper complex is copper concentration dependent as expected (for comparison see figure 4Sb)

Moreover, MS/MS experiments for the peaks at *m/z* 1121.4 (BK-Cu 1:1 complex) and 1122.4 (BK-Zn 1:1 complex) show different features (see figure 8S). Particularly, in the case of BK-Cu complex a fragment at m/z 1077.2 (loss of 44 uma, a carboxylic group) is very abundant and easily formed even at low collision energy, while this is not the case for the BK-Zn complex, hinting different coordination features with carboxylic groups for the two complexes. In the case of the BK-Cu, MS/MS experiments show also a loss of 143.1 uma ($NHCHCOOCH_2CH_2CH_2CH_2NH$) to produce the 978.1 uma fragment, not present in the case of BK-Zn. A detailed MS analysis of possible copper(I) and copper(II) coordination features has been already reported in the literature[46] and repeating such analysis here would be redundant. However, in our knowledge the effect of copper and zinc ions on BK oligomerization has never been reported. Surprisingly, figure 5S and figure 6S indicate that the effect of the two metal ions on the BK oligomerization might be different. Indeed, MS detection of BK_2Zn and BK_3Zn species (figure 5S and Table 1) points to the presence of oligomeric species in the presence of zinc ions, while in the presence of copper ions the detection of these species is remarkably hindered in a concentration dependent manner (see figure 6S).

Circular Dichroism

To better investigate the oligomerization features of BK solutions at different concentrations suggested by the MS results and how these are affected by the presence of copper and zinc ions, we have performed CD experiments. Panel A of figure 1 reports the far-UV CD spectra of BK recorded in pure water at pH 6.5, room temperature and at a 35 μM of peptide concentration (solid line). CD spectra show two weak dichroic signals, a positive one centred at 223 nm, a negative one at 235 nm, and an intense negative band at 204 nm. These CD bands are typical of a type II poly-L-proline left-handed extended helix (PPII).[47,48] The intensities and the positions of the CD bands, in the 35-100 μM range do not depend on peptide concentrations (see solid lines of panels A and B). The CD curves recorded at 35 μM of peptide concentration are not affected by a twofold excess of Cu(II) (dashed lines) or Zn(II) (dotted lines) ions. The CD spectrum of BK was insensitive to the presence of excess Zn(II) also at higher peptide concentrations (100 μM). By contrast, the addition of a twofold excess of Cu(II) ions to BK 100 μM induced a fourfold and threefold enhancement of the intensities of CD minima observed at 204 and 234 nm respectively, but no significant deviations of the positive band at 222 nm (figure 1, panel B, dashed line). Cu(II)-induced changes of CD spectra of BK are evidenced only at high copper concentration, and this is accordance with a perturbed association/dissociation equilibrium. In a previous report, the negative CD band observed at 234 nm for apo-BK was attributed to internally hydrogen-bonded Pro7 residues.[49] However, in those early experiments CD spectra were recorded at acidic pH, in which dimeric peptide structure are unlikely to form. By contrast, our experiments were performed at neutral pH, and in these conditions dimeric or trimeric peptide assemblies are always present as evidenced from ESI-MS results experiments. Due to the hydrophobic nature of the C-terminal segment of the peptide it is plausible that peptide association occur by intermolecular Phe-Phe interactions which, in turn, is expected to disrupt the H-bridged structures involving Pro7 residues. This reconciles with CD spectra reported in the present work in which a very weak negative CD band at 234 nm is observed. Notably, this band increases in the presence of high copper concentrations. This means that copper may promote BK-dissociation into monomers with a consequent increase of the negative band at 234 nm in

accordance with ESI-MS results and molecular simulations. Moreover, copper-dependent peptide dissociation is likely to occur with a consequent increase of the structural disorder as evidenced by the increase of the negative band centered at 205 nm.

Computational analysis

The structural motivations behind the two different effects of copper(II) and zinc(II) metal ions on BK oligomerization were also investigated by computational analysis as described in the experimental section. An accurate sampling of the BK conformations was initially carried out through Parallel Tempering simulations.[50] We selected the main clusters which are equally populated and from those we back calculated the CD spectra. The latter show a nice agreement with those experimentally recorded, confirming the presence of type II poly-L-proline left-handed extended helix (PPII) (see figure 9S).

From those conformations, zinc and copper were coordinated to BK in accordance with the ESI/MS indications and the coordination polyhedral were predicted in the DFT framework. The coordination shell is saturated through two coordination waters. The coordination polyhedron moves towards a planar arrangement upon BK binding to copper(II). In these regards, BK coordinates with copper(II) via the C-terminal carboxyl oxygen of asparagine, the carbonyl oxygen of the N-terminal asparagine and two inner sphere water molecules. The carbonyl oxygen belonging to the N-terminal Arg competes with the N-terminal amine group for the fourth coordination position (figure 2b, Table 2), indeed one among the preferred ligand for copper(II).[51,52]

In line with the results obtained by MS and CD analysis, upon a double excess of BK with respect to zinc ion, an elongated peptide conformation is stabilized with a head-to-tail coordination polyhedron (Figure 2c). Here, Zn^{2+} is coordinated to the two carboxylic groups of BK and two coordination waters (Table 2). The C-terminal Arg weakly contacts the uncoordinated carboxylic oxygen of a different BK unit (Figure 2c). However, upon a double excess of BK with respect to copper(II) ion, the monomeric complex of copper(II) is still formed (Figures 2b and 2d) leaving

uncomplexed one peptide unit of BK. This indicates an unfavourable geometry experienced by copper(II) upon coordinating two BK units, since the requirement of a planar coordination polyhedron. A dimeric structure can instead formed through the coordination of zinc ion, since the coordination polyhedron is favoured by a tetrahedral spatial arrangement (Figure 2c).

Enzymatic degradation assay

We have also assessed if the presence of metal ions affects BK proneness to degradation by IDE. This enzyme was selected among all the available BK degrading enzymes because of its involvement with AD and the deep knowledge of IDE degrading activity towards various substrates by our group.[53-59] In figure 10S of the Supplementary information the mass spectra recorded after BK incubation with IDE in the presence and in the absence of copper and zinc ions are reported. According to previously published results,[22,60] also in this case, copper(II) strongly inhibits IDE activity (by binding directly to the enzyme), while zinc(II), differently from other IDE substrates such as amylin,[61] does not affect BK fragmentation pattern. This result is in line with our binding model, according to which zinc does not affect BK conformation and therefore its proneness to degradation.

Biochemical analysis

The oligopeptide BK, produced after cleavage of kininogens by kallikreins in the plasma or interstitial fluid, triggers its effects by the activation of two G protein coupled transmembrane receptors, called B_1R and B_2R.[62] B_1R is generally absent or under-expressed in physiological conditions, has high affinity for kinin metabolites (des-^{9}Arg-BK and ^{8}Leu-des-^{9}Arg-BK), and is upregulated to mediate inflammatory conditions following tissue injury or under pathological states. Conversely, B_2R is a constitutive receptor that displays higher affinity for BK (and Kallidin) peptide, is widely distributed and mediates most biological effects of kinins.[63]

The expression of both receptors has shown to increase in the brains of Aβ1-40 treated rats,[64] whereas the blockade of B_2R has been reported to be beneficial on cognitive deficit induced by Aβ1-40.[65,66] Therefore it is clear that any intervention that could affect the binding activity on these receptors can produce beneficial effects against inflammatory neurodegenerative diseases. The activated signalling pathway goes through Erk phosphorylation and leads to up-regulation of pro-inflammatory molecules such as IL-1beta. Thus we tested the effects of metal ions (copper and zinc) on BK activity by analysing phosphorylation and expression of these two markers respectively. For this investigation we used the human monocytic THP-1 cell line as innate immunity model system and we examined the BK effects on normal THP-1 with monocytic phenotype or on activated THP-1 that shows a stronger pro-inflammatory response as result of B_1R up-regulation.[67] THP-1 is a human leukemic cell line with monocytic nature that can be pathogenically challenged to initiate an inflammatory response. LPS stimulated THP-1 cells incubated with the bacterial endotoxin, lipopolysaccharide (LPS), can produce an inflammatory response with increase of IL-1β secretion through a PKA-dependent mechanism.[68]

To ascertain any toxic effect of BK, a dose response experiment was first performed to test the cell viability after treatment with BK, BK-Cu(II) and Cu(II) using a range of concentrations known to be effective. The cell cultures were fully viable at all concentrations used allowing further tests at the higher dosage (figure 3). ERK phosphorylation is considered a good marker of neuroinflammatory signalling cascade activation,[69] and was thus analyzed in cell cultures treated with different preparations of BK.

Undifferentiated monocyte cell cultures were treated with the higher not toxic dose of BK alone (50μM), BK preincubated in combination with copper or zinc (1 hour, ratio 1:2) or with 0.5μg/ml LPS as positive control. After 15 min of treatments the Western blot analyses of phosphorylated ERK (pERK) showed a weak cell culture response. However it was possible to measure a 70% increase of pERK after 15 minutes of BK treatment, that was abolished by BK preincubation with two fold copper (100μM, 1 hour) and only partially by BK preincubation with zinc (figure 4A).

Moreover, to verify whether the effects on signalling cascade are followed by corresponding effects on pro-inflammatory cytokines synthesis, we performed the analyses of IL-1 beta expression after 20 hours of treatment. As expected, the western blot analyses showed an up-regulation in the presence of BK (+100%) and this effect was counteracted by BK preincubation with metals, particularly with copper (figure 4B).

The treatments of pre-activated THP-1 monocytes, that typically show a macrophagic phenotype, more clearly reproduced the observed effects. Indeed we measured a more intense BK induction of ERK phosphorylation (+100%), and this effect was strongly reduced after treatment with BK preincubated with copper. The minor effect of the BK preincubated in the presence of zinc, with respect to the presence of copper, was again observed, thus confirmed (figure 5A). Similarly IL-1beta up-regulation by treatment with BK (+500%) was abolished by preincubation of BK in the presence of copper, but only weakly inhibited in the presence of zinc (figure 5B).

Discussion

We have observed two different effects of copper(II) and zinc(II) metal ions on BK conformation and oligomerization. MS and CD experiments indicate that copper(II), differently from zinc(II), is able to hinder BK oligomerization and the results are in line with the computational analysis.

The biochemical data support the hypothesis that conformational changes observed upon copper/BK binding are responsible of significant differences of the metal effects on proinflammatory activity of BK.

Several evidences support the notion of Kallikrein-Kinin System (KKS) involvement in AD. The contact/kinin system is activated in cerebrospinal fluid (CSF) of patients with AD by the cleavage of high molecular mass kininogen, providing the link between the KKS and the pathogenesis of AD.[70,71] This correlation has been also supported by the observation that Aβ peptides infusion can trigger an increase in kinin concentration in the cerebrospinal fluid of animals, proving that an

enhanced activation of KKS takes part in the inflammatory driven toxicity in AD.[72] In this respect, amongst the mechanisms that are altered in AD, activation of KKS has been correlated to up-regulation of bradykinin receptors,[73] secretion of the amyloid precursor protein,[74] and activation of MAPK, Erk1 and Erk2 phosphorylation, a mechanism found to early distinguish AD from other dementias.[69]

Here we demonstrated that copper binding can change BK conformation and this in turn can challenge a BK signalling fault, measured as reduction in Erk1/2 phosphorylation and IL-1β expression, that is likely related to failure or defective BK binding to its receptors. This is indeed evidenced by the more intense and significant effects observed on THP-1 differentiated cells which present a typical macrophagic phenotype, and higher BK receptors expression hence.[75]

AD is the most concerned neurodegenerative disease with respect to copper levels and effects on the specific Aβ peptide conformational changes, including in particular the inflammatory status that significantly contributes to the progression and effects of this devastating disease. Indeed, new data from preclinical and clinical studies have established that immune system-mediated actions in fact contribute to and drive AD pathogenesis. These insights have suggested both novel and well-defined potential therapeutic targets for AD, including microglia and several cytokines.[76] Nonetheless, we didn't find direct effects of BK on Aβ toxicity (see suppl. 11S), but the significant copper effects on BK conformation and activity observed herein provide a new perspective on the consequences of copper dishomeostasis in those neurodegenerative diseases, like AD, where the effects of protein misfolding are associated to an inflammatory status, now recognized to be not simply a collateral condition.

Conclusions

In this work we have been able to correlate a metal induced effect on BK conformation and oligomerization with a change in BK activity measured as reduction in Erk1/2 phosphorylation and IL-1β expression, that is likely related to failure or defective BK binding to its receptors.

BK is known to be involved in many crucial biological processes, but here particular attention has been devoted to its role in chronic inflammatory diseases, included neurodegenerative diseases like AD. Since copper, and more generally metals, dyshomeostasis has been claimed to be responsible of several related complains, the copper effects on BK conformation and activity observed herein can open new potentiality in the treatment of neuroinflammatory diseases by management of copper level and distribution.

Acknowledgements

We thank PRIN 2008R23Z7K and FIR 2014 9DD800 for financial support.

Tables

BK species	Experimental (*m/z*)	Calculated Isotopic (*m/z*)
3BK + ArgPhe – C_6H_6 + H^+	3422.8	3422.9
3BK + $CH_2CH_2CH_2NHCNHNH$ – H^+ + Zn^{2+}	3340.7	3340.7
3BK + $CH_2CH_2CH_2NHCNHNH$ – H^+ + Cu^{2+}	3339.7	3339.7
3BK + $CH_2CH_2CH_2NHCNHNH$ + H^+	3278.6	3278.8
3BK + H^+	3179.7	3179.7
2BK + ArgPhe – C_6H_6 + H^+	2363.0	2363.3
2BK + 2Zn^{2+} + $CH_2CH_2CH_2NHCNH_2NH_2$ – 3H^+	2345.0	2345.0

$2BK + Zn^{2+} + CH_2CH_2CH_2NHCNHNH_2 - H^+$	2282.1	2282.1
$2BK + Cu^{2+} + CH_2CH_2CH_2NHCNHNH_2 - H^+$	2281.1	2281.1
$2BK + CH_2CH_2CH_2NHCNHNH + H^+$	2219.0	2219.2
$2BK + Zn^{2+} - H^+$	2182.1	2182.0
$2BK + H^+$	2120.3	2120.1
$BK + Zn^{2+} - H^+ + CH_2CH_2CH_2NHCNHN$	1220.2	1220.5
$BK + Cu^{2+} - H^+ + CH_2CH_2CH_2NHCNHN$	1219.3	1219.5
$BK + Arg - H_2O - 4H + H^+$	1212.1	1212.7
$BK + Zn^{2+} - H^+$	1122.4	1122.5
$BK + Cu^{2+} - H^+$	1121.4	1121.5
$BK + Na^+$	1082.5	1082.5
$BK + H^+$	1060.5	1060.6
$ArgProProGlyPheSerProPhe + H^+$	904.4	904.4
$BK + Arg - H_2O - 4H + 2H^+$	606.6	607.3
$BK + Cu^{2+}$	561.2	561.2
$BK + 2H^+$	530.9	530.8
$BK + H^+ + Na^+$	541.8	541.8
$BK + 2H^+ + K^+$	367.0	366.7
$BK + 3H^+$	354.1	354.2
$BK + Zn^{2+} + H^+$	374.8	374.8
$BK + Cu^{2+} + H^+$	374.5	374.5

Table 1

Zn^{2+}-BK			
Bond	**Bond length (Å)**	**Angle type**	**Angle (degree)**
Zn^{2+}-NH_2	2.17	OH_2-Zn^{2+}-NH_2	117.88
Zn^{2+}-OCO	1.97	OH_2-Zn^{2+}-NH_2	115.19
Zn^{2+}-OH_2	2.09	OH_2-Zn^{2+}- OH_2	119.79
Zn^{2+}-OH_2	2.09	OH_2-Zn^{2+}-OCO	97.23
Cu^{2+}-BK			
Bond	**Bond length (Å)**	**Angle type**	**Angle (degree)**
Cu^{2+}-NH_2	2.35	NH_2 -Cu-OH_2	104.08
Cu^{2+}-OC	2.02	OH_2-Cu^{2+}-OC	95.92
Cu^{2+}-OCO	1.95	OH_2-Cu^{2+}-OC	82.10
Cu^{2+}-OH_2	2.02	OH_2-Cu^{2+}- OH_2	139.54
Cu^{2+}-OH_2	2.03	OH_2-Cu^{2+}-OCO	91.75
Zn^{2+}-$(BK)_2$			
Bond	**Bond length (Å)**	**Angle type**	**Angle (degree)**
Zn^{2+}-OCO	1.94	OH_2-Zn^{2+}-OCO	108.13
Zn^{2+}-OCO	1.91	OH_2-Zn^{2+}-OCO	104.62
Zn^{2+}-OH_2	2.06	OH_2-Zn^{2+}- OH_2	103.22
Zn^{2+}-OH_2	2.07	OCO-Zn^{2+}-OCO	129.43

Table 2

References

[1] P. Kaur, A. Muthuraman and M. Kaur, The implications of angiotensin-converting enzymes and their modulators in neurodegenerative disorders: current and future perspectives, *ACS Chem. Neurosci.* 2015, **6**, 508–521.

[2] N.P. Mason, M. Petersen, C. Mélot, E.V. Kim, A. Aldashev, A. Sarybaev, M.M. Mirrakhimov and R. Naeije, Changes in plasma bradykinin concentration and citric acid cough threshold at high altitude, *Wilderness Environ. Med.* 2009, **20**, 353–358.

[3] L.R. Dalemar, Y.J. Ivy Jong, B. Wilhelm and N.L. Baenziger, Protein kinases A and C rapidly modulate expression of human lung fibroblast B2 bradykinin receptor affinity forms, *Eur. J. Cell Biol.* 1996, **69**, 236–244.

[4] B. Lacoste, X.-K. Tong, K. Lahjouji, R. Couture and E. Hamel, Cognitive and cerebrovascular improvements following kinin B1 receptor blockade in Alzheimer's disease mice, *J. Neuroinflammation* 2013, **10**, 57.

[5] F.A. Amaral, M.T.R. Lemos, K.E. Dong, M.F.Q.P. Bittencourt, A.L. Caetano, J.B. Pesquero, T.A. Viel and H.S. Buck, Participation of kinin receptors on memory impairment after chronic infusion of human amyloid-β 1-40 peptide in mice. *Neuropeptides* 2010, **44**, 93–97.

[6] C.M. Costa-Neto, P. Dillenburg-Pilla, T.A. Heinrich, L.T. Parreiras-e-Silva, M.G. Pereira, R.I. Reis and P.P.C. Souza, Participation of kallikrein-kinin system in different pathologies, *Int. Immunopharmacol.* 2008, **8**, 135–142.

[7] K. Walker, M. Perkins and A. Dray, Kinins and kinin receptors in the nervous system, *Neuroch. Int.* 1995, **26**, 1–26.

[8] T.A. Viel and H.S. Buck, Kallikrein-Kinin system mediated inflammation in Alzheimer's disease in vivo, *Cur. Alzheimer Res.* 2011, **8**, 59–66.

[9] L.M. Iores-Marçal, T.A. Viel, H.S. Buck, V.A. Nunes, A.J. Gozzo, I. Cruz-Silva, A. Miranda, K. Shimamoto, N. Ura and M.S. Araujo, Bradykinin release and inactivation in brain of rats submitted to an experimental model of Alzheimer's disease, *Peptides* 2006, **27**, 3363–3369.

[10] E. Malito, L.A. Ralat, M. Manolopoulou, J.L. Tsay, N.L. Wadlington and W.-J. Tang, Molecular bases for the recognition of short peptide substrates and cysteine-directed modifications of human insulin-degrading enzyme, *Biochemistry* 2008, **47**, 12822–12834.

[11] G. Grasso, P. Mielczarek, M. Niedziolka and J. Silberring, Metabolism of cryptic peptides derived from neuropeptide FF precursors: the involvement of insulin-degrading enzyme, *Int. J. Mol. Sci.* 2014, **15**, 16787–16799.

[12] D.K. Lahiri, D.M. Chen, P. Lahiri, S. Bondy and G. H. Greig, Amyloid, cholinesterase, melatonin, and metals and their roles in aging and neurodegenerative diseases, *Ann. N. Y. Acad. Sci*., 2005, **1056**, 430–449.

[13] M.A. Lovell, J.D. Robertson, W.J. Teesdale, J.L. Campbell and W.R. Markesbery, Copper, iron and zinc in Alzheimer's disease senile plaques, *J. Neurol. Sci*., 1998, **158**, 47–52.

[14] P.J. Crouch and K.J. Barnham. Therapeutic redistribution of metal ions to treat Alzheimer's disease. *Acc. Chem. Res.* 2012, **45**, 1604–1611.

[15] P.A. Adlard, L. Bica, A.R. White, M. Nurjono, G. Filiz, P.J. Crouch, P.S. Donnelly, R, Cappai, D.I. Finkelstein and A.I. Bush. Metal ionophore treatment restores dendritic spine density and synaptic protein levels in a mouse model of Alzheimer's disease. *PLoS One*2011, **6**, e17669.

[16] P. Lei, S. Ayton, A.T. Appukuttan, I. Volitakis, P.A. Adlard, D.I. Finkelstein and A.I. Bush. Clioquinol rescues Parkinsonism and dementia phenotypes of the tau knockout mouse. *Neurobiol. Dis*. 2015, **81**, 168–175.

[17] A. I. Bush and R. E. Tanzi, Therapeutic for Alzheimer's disease based on the metal hypothesis, *Neurotherapeutics*, 2008, **5**, 421–432.

[18] G. Arena, R. Fattorusso, G. Grasso, G.I. Grasso, C. Isernia, G. Malgieri, D. Milardi and E. Rizzarelli. Zinc(II) complexes with ubiquitin: speciation, affinity and binding features. *Chem.- Eur. J.* 2011, **17**, 11596–11603.

[19] D. Milardi, F. Arnesano, G. Grasso, A. Magrì, G. Tabbì, S. Scintilla, G. Natile, Ubiquitin stability and the Lys 63 linked polyubiquitination site are compromised on copper binding, *Angew. Chem. Int. Edit.* 2007, **46**, 7993–7995.

[20] G. Arena, F. Bellia, G. Frasca, G. Grasso, V. Lanza, E. Rizzarelli and G. Tabbì, Inorganic stressors of ubiquitin, *Inorg. Chem*. 2013, **52**, 9567–9573.

[21] A. Travaglia, D. La Mendola, A. Magrì, A. Pietropaolo, V.G. Nicoletti, G. Grasso, G. Malgieri, R. Fattorusso, C. Isernia and E. Rizzarelli. Zn(II) interactions with BDNF N-terminal peptide fragments: inorganic features and biological perspectives. *Inorg. Chem*. 2013, **52**, 11075–11083.

[22] G. Grasso, A. Pietropaolo, G. Spoto, G. Pappalardo, G.R. Tundo, C. Ciaccio, M. Coletta and E. Rizzarelli, Copper(I) and copper(II) inhibit Aβ peptides proteolysis by insulin-degrading enzyme differently: implications for metallostasis alteration in Alzheimer's disease, *Chem.- Eur. J.* 2011, **17**, 2752–2762.

[23] B. Ivanova and M. Spiteller, Coordination ability of bradykinin with ZnII- and AgI-metal ions – Experimental and theoretical study, *Inorg. Chimica Acta* 2012, **392**, 211–220.

[24] M. Prudent and H.H. Girault, On-line electrogeneration of copper–peptide complexes in microspray mass spectrometry, *J. Am. Soc. Mass Spectrom.* 2008, **19**, 560–568.

[25] J. Dong, R.W. Vachet, Coordination sphere tuning of the electron transfer dissociation behavior of Cu(II)–peptide complexes, *J. Am. Soc. Mass Spectrom*. 2012, **23**, 321–329.

[26] B.A. Cerda, L. Cornett and C. Wesdemiotis, Probing the interaction of alkali and transition metal ions with bradykinin and its des-arginine derivatives via matrix-assisted laser desorption/ionization and postsource decay mass spectrometry, *Int. J. Mass Spectrom*. 1999, **193**, 205–226.

[27] G. Malgieri and G. Grasso, The clearance of misfolded proteins in neurodegenerative diseases by zinc metalloproteases: an inorganic perspective, *Coordin. Chem. Rev.* 2014, **260**, 139–155.

[28] B. Hess, C. Kutzner, D. van der Spoel and D. Lindahl, GROMACS 4: algorithms for highly efficient, load-balanced, and scalable molecular simulation, *J. Chem. Theory Comp*. 2008, **4**, 435–447.

[29] V. Hornak, R. Abel, A. Okur, B. Strockbine, A. Roitberg and C. Simmerling, Comparison of multiple Amber force fields and development of improved protein backbone parameters, *Proteins* 2006, **65**, 712–725.

[30] W.L. Jorgensen, J. Chandrasekhar, J.D. Madura, R.W. Impey and M.L. Klein, Comparison of simple potential functions for simulating liquid water, *J. Chem. Phys*. 1983, **79**, 926–935.

[31] U. Essmann, L. Perera, M.L. Berkowitz, T. Darden, H. Lee and L.G. Pedersen, A smooth particle mesh Ewald method, *J. Chem. Phys*. 1995, **103**, 8577–8593.

[32] S. Miyamoto and P.A. Kollman, SETTLE: an analytical version of the SHAKE and RATTLE algorithms for rigid water models, *J. Comp. Chem*. 1992, **13**, 952–962.

[33] B. Hess, P-LINCS: A parallel linear constraint solver for molecular simulation, *J. Chem. Theory Comput.* 2008, **4**, 116–122.

[34] G. Bussi, D. Donadio and M. Parrinello, Canonical sampling through velocity rescaling, *J. Chem. Phys.* 2007, **126**, 014101.

[35] E. Rosta, N.V. Buchete and G. Hummer. Thermostat artifacts in replica exchange molecular dynamics simulations. *J. Chem. Theory Comput.* 2009, **5**, 1393–1399.

[36] X. Daura, K. Gademann, B. Jaun, D. Seebach, W.F. van Gunsteren and A.E. Mark, Peptide folding: when simulation meets experiment, *Angew. Chem. Int. Edit.* 1999, **38**, 236–240.

[37] Gaussian 09, Revision D.01, M.J. Frisch et al. *Gaussian, Inc., Wallingford CT*, 2009.

[38] B.M. Bulheller and J.D. Hirst, DichroCalc -Circular and Linear Dichroism Online, *Bioinformatics*, 2009, **25**, 539–540.

[39] L. Gianelli, V. Amendola, L. Fabbrizzi, P. Pallavicini and G. Mellerio, Investigation of reduction of Cu(II) complexes in positive-ion mode electrospray mass spectrometry, *Rapid Commun. Mass Spectrom.* 2001, **15**, 2347–2353.

[40] D. Grasso, C. La Rosa, D. Milardi and S. Fasone, The effects of scan rate and protein concentration on DSC thermograms of bovine superoxide dismutase, *Thermochimica Acta* 1995, **265**, 163–175.

[41] L. Zhou, L.H. Shen, L.H. Hu, H. Ge, J. Pu, D.j. Chai, Q. Shao, L. Wang, J.Z. Zeng and B. He, Retinoid X receptor agonists inhibit phorbol-12-mystrate-13-acetate (PMA)-induced differentiation of monocytic THP-1 cells into macrophages. *Mol. Cell. Biochem*. 2009, **335**, 283–289.

[42] E.J. Nettleton, P. Tito, M. Sunde, M. Bouchard, C.M. Dobson and C.V. Robinson, Characterization of the oligomeric states of insulin in self-assembly and amyloid fibril formation by mass spectrometry. *Biophys J.* 2000, **79**, 1053–1065.

[43] C. Lifshitz, A review of gas-phase H/D exchange experiments: the protonated arginine dimer and bradykinin nonapeptide systems, *Int. J. Mass Spectrom*. 2004, **234**, 63–70.

[44] Z.L. Cheng, K.W.M. Siu, R. Guevremont and S.S. Berman, Electrospray mass spectrometry: a study on some aqueous solutions of metal salts, *J. Am. Soc. Mass Spectrom*. 1992, **3**, 281–288.

[45] G. Grasso, A. Magrì, F. Bellia, A. Pietropaolo, D. La Mendola and E. Rizzarelli, The copper(II) and zinc(II) coordination mode of HExxH and HxxEH motif in small peptides: the role of carboxylate location and hydrogen bonding network, *J. Inorg. Biochem.* 2014, **130**, 92–102.

[46] M. Prudent and H. H. Girault, On-line electrogeneration of copper–peptide complexes in microspray mass spectrometry, *J. Am. Soc. Mass Spectrom.* 2008, **19**, 560–568.

[47] A.S. Tatham, A.F. Drake and P.R. Shewry, Conformational studies of a synthetic peptide corresponding to the repeat motif of C hordein, *Biochem. J.* 1989, **259**, 471–476.

[48] G. Di Natale, G. Pappalardo, D. Milardi, M.F.M. Sciacca, F. Attanasio, D. La Mendola and E. Rizzarelli, Membrane interactions and conformational preferences of human and avian prion N-

terminal tandem repeats: the role of copper(II) ions, pH, and membrane mimicking environments, *J. Phys. Chem. B* 2010, **114**, 13830–13838.

[49] J.R. Cann, J.M. Stewart and G.R. Matsueda, A circular dichroism study of the secondary structure of bradykinin. *Biochemistry* 1973, **12**, 3780–3788.

[50] Y. Sugita and Y. Okamoto. Replica-exchange molecular dynamics method for protein folding. *Chem. Phys. Lett.* 1999, **314**, 141–151.

[51] A. Travaglia, D. La Mendola, A. Magrì, V.G. Nicoletti, A. Pietropaolo and E. Rizzarelli. Copper, BDNF and its N-terminal domain: inorganic features and biological perspectives. *Chem. Eur. J.* 2012, **18**, 15618–15631.

[52] R. De Ricco, D. Valensin, S. Dell'Acqua, L. Casella L, P. Dorlet P, P. Faller and C. Hureau. Remote His50 acts as a coordination switch in the high-affinity N-terminal centered copper(II) site of α-synuclein. *Inorg. Chem.* 2015, **54**, 4744–4751.

53 F. Bellia, A. Pietropaolo and G. Grasso, Formation of insulin fragments by insulin-degrading enzyme: the role of zinc(II) and cystine bridges. *J. Mass Spectrom*. 2013, **48**, 135–140

[54] G. Grasso, E. Rizzarelli and G. Spoto, The proteolytic activity of insulin-degrading enzyme: a mass spectrometry study. *J. Mass Spectrom*. 2009, **44**, 735–741.

[55] C. Ciaccio, G.F. Tundo, G. Grasso, G. Spoto, D. Marasco, M. Ruvo, S. Marini, E. Rizzarelli and M. Coletta, Somatostatin: a novel substrate and a modulator of insulin degrading enzyme activity. *J. Mol. Biol.* 2009, **385**, 1556–1567.

[56] G. Grasso, A.I. Bush, R. D'Agata, E. Rizzarelli and G. Spoto, Enzyme solid-state support assays: a surface plasmon resonance and mass spectrometry coupled study of immobilized insulin degrading enzyme. *Eur. Biophys. J.* 2009, **38**, 407–414.

[57] G. Grasso, E. Rizzarelli and G. Spoto, How the binding and degrading capabilities of insulin degrading enzyme are affected by ubiquitin. *BBA-Proteins and Proteomics* 2008, **1784**, 1122–1126.

[58] G. Grasso, E. Rizzarelli and G. Spoto, AP-MALDI/MS complete characterization of insulin fragments produced by the interaction of IDE with bovine insulin. *J. Mass Spectrom*. 2007, **42**, 1590–1598.

[59] G. Grasso, C. Satriano and D. Milardi, A neglected modulator of insulin-degrading enzyme activity and conformation: the pH. *Biophys. Chem.* 2015, **203-204**, 33–40.

[60] G. Grasso, F. Salomone, G.R. Tundo, G. Pappalardo, C. Ciaccio, G. Spoto, A. Pietropaolo, M. Coletta and E. Rizzarelli, Metal ions affect insulin-degrading enzyme activity, *J. Inorg. Biochem*. 2012, **117**, 351–358.

[61] F. Bellia and G. Grasso, The role of copper(II) and zinc(II) in the degradation of human and murine IAPP by insulin-degrading enzyme, J. Mass Spectrom. 2014, **49**, 274–279.

[62] D. Regoli and J. Barabe, Pharmacology of bradykinin and related kinins, *Pharmacol. Rev.* 1980, **32**, 1–46.

[63] S.A. Mathis, N.L. Criscimagna and L.M.F. Leeb-Lundberg, B1 and B2 kinin receptors mediate distinct patterns of intracellular Ca^{2+} signaling in single cultured vascular smooth muscle cells. *Mol. Pharmacol*. 1996, **50**, 128–139.

[64] T.A. Viel, A. Lima Caetano, A.G. Nasello, C.L. Lancelotti, V.A. Nunes, M.S. Araujo and H.S. Buck, Increases of kinin B1 and B2 receptors binding sites after brain infusion of amyloid-beta 1–40 peptide in rats. *Neurobiol. Aging* 2008, **29**,1805–1814.

[65] R.D. Prediger, R. Medeiros, P. Pandolfo, F.S. Duarte, G.F. Passos, J.B. Pesquero, M.M. Campos, J.B. Calixto and R.N. Takahashi. Genetic deletion or antagonism of kinin B(1) and B(2) receptors improves cognitive deficits in a mouse model of Alzheimer's disease. *Neuroscience* 2008, **151**, 631–643.

[66] M.A. Bicca, R. Costa, G. Loch-Neckel, C.P. Figueiredo, R. Medeiros and J.B. Calixto. B2 receptor blockage prevents Aβ-induced cognitive impairment by neuroinflammation inhibition *Behav. Brain Res.* 2015, **278**, 482–491.

[67] S. Tsuchiya, M. Yamabe, Y. Yamaguchi, Y. Kobayashi, T. Konno and K. Tada. Establishment and characterization of a human acute monocytic leukemia cell line (THP-1). *Int. J. Cancer*. 1980, **26**, 171–176.

[68] L.A. Grisanti, J. Evanson, E. Marchus, H. Jorissen, A.P. Woster, W. DeKrey, E.R. Sauter, C.K. Combs and J.E. Porter. Pro-inflammatory responses in human monocytes are β1-adrenergic receptor subtype dependent. *Mol. Immunol.* 2010, **47**, 1244–1254.

[69] T.K. Khan and D.L. Alkon. An internally controlled peripheral biomarker for Alzheimer's disease: Erk1 and Erk2 responses to the inflammatory signal bradykinin. *Proc. Natl. Acad. Sci.* 2006, **103**, 13203–13207.

[70] L. Bergamaschini, C. Donarini, G. Gobbo, L. Parnetti and V. Gallai. Activation of complement and contact system in Alzheimer's disease. *Mech. Ageing Dev.* 2001, **122**, 1971–1983.

[71] T.A. Viel and H.S. Buck. Abeta and BK kallikrein-kinin system mediated inflammation in Alzheimer's disease in vivo. *Curr. Alzheimer Res.*, 2011, **8**, 59–66.

[72] L.M. Iores-Marçal, T.A. Viel, H.S. Buck, V.A. Nunes, A.J. Gozzo, I. Cruz-Silva, A. Miranda, K. Shimamoto, N. Ura and M.S. Araujo. Bradykinin release and inactivation in brain of rats submitted to an experimental model of Alzheimer's disease. *Peptides* 2006, **27**, 3363–3369.

[73] H.M. Huang, T.A. Lin, G.Y. Sun and G.E. Gibson. Increased inositol 1,4,5-Trisphosphate accumulation correlates with an up-regulation of bradykinin receptors in Alzheimer's disease. *J. Neurochem*. 1995, **64**, 761–766.

[74] R.M. Nitsch, C. Kim and J.H. Growdon. Vasopressin and bradykinin regulate secretory processing of the amyloid protein precursor of Alzheimer's disease. *Neurochem. Res.* 1998, **23**, 807–814.

[75] C.M. Bertram, S. Baltic, N.L. Misso, K.D. Bhoola, P.S. Foster, P.J. Thompson and M. Fogel-Petrovic. Expression of kinin B1 and B2 receptors in immature, monocyte-derived dendritic cells

and bradykinin-mediated increase in intracellular Ca^{2+} and cell migration. *J. Leukoc. Biol*. 2007, **81**, 1445–1454.

[76] F.L. Heppner, R.M. Ransohoff and B. Becher. Immune attack: the role of inflammation in Alzheimer disease. *Nat. Rev. Neurosci*. 2015, **16**, 358–372.

Figure and Table Legends

Table 1: Experimental and calculated m/z values for the BK species detected by ESI-MS from BK solutions at various concentrations with and without metal ions (Cu^{2+} and Zn^{2+}). Assignment of the peak at m/z 904.4 has been confirmed by MS/MS experiments that allow to exclude the presence of the isobar peptide HPro-Pro-Gly-Phe-Ser-Pro-Phe-ArgOH.

Table 2: Coordination parameters for the Zn^{2+} and Cu^{2+} optimized complexes with BK. Root mean square displacement during geometry optimization is 10^{-3} Å.

Figure 1: The effect of Cu(II) and Zn(II) ions on the CD signals of BK in water at neutral pH and different peptide concentrations. CD spectra of 35 μM (panel A) and 100 μM (panel B) of pure BK (solid lines) and in the presence of a twofold excess of Cu(II) (dashed lines) or Zn(II) (dotted lines) ions.

Figure 2: a) Coordination structure of Zn^{2+} complex with BK. b) Coordination structure of Cu^{2+} complex with BK. c) Coordination structure of the dimeric complex of Zn^{2+} with BK. The weak interaction between the C-terminal Arg and the carboxylic oxygen is circled. d) No dimer formation occurs with a 1:2 stoichiometric ratio of Cu^{2+} and BK.

Figure 3: Dose response experiment to test the cell viability after treatment with BK, BK-Cu(II) and Cu(II). THP-1 cell cultures (undifferentiated monocytes) were incubated with increasing concentrations of BK and BK-Cu(II) for 20h and then cell viability was measured using MTT assay. Results are presented as the means ± SEM, the experiments were performed 3 times in triplicate.

Figure 4: Expression of A) pErk1/2 and B) IL-1 beta in THP-1 cell cultures (undifferentiated monocytes) after 15 min and 20 hrs of treatment, respectively, with BK, copper or zinc alone, or BK pre-incubated with metals (1 h, ratio 1:2). Results are presented as mean ±SEM, the experiments were performed 3 times in triplicate. Asterisk (*) represents the correlation significant at the $p \leq 0.05$ level w.r.t. control, One-way Anova.

Figure 5: Expression of A) pErk1/2 and B) IL-1 beta in THP-1 cell cultures (differentiated monocytes: macrophages) after 15 min and 20 hrs of treatment, respectively, with BK or BK pre-incubated with copper or zinc (1 h, ratio 1:2). Results are presented as mean ±SEM, the experiments were performed 3 times in triplicate. Asterisk (*) represents the correlation significant at the $p \leq 0.05$ level w.r.t. control, One-way Anova.

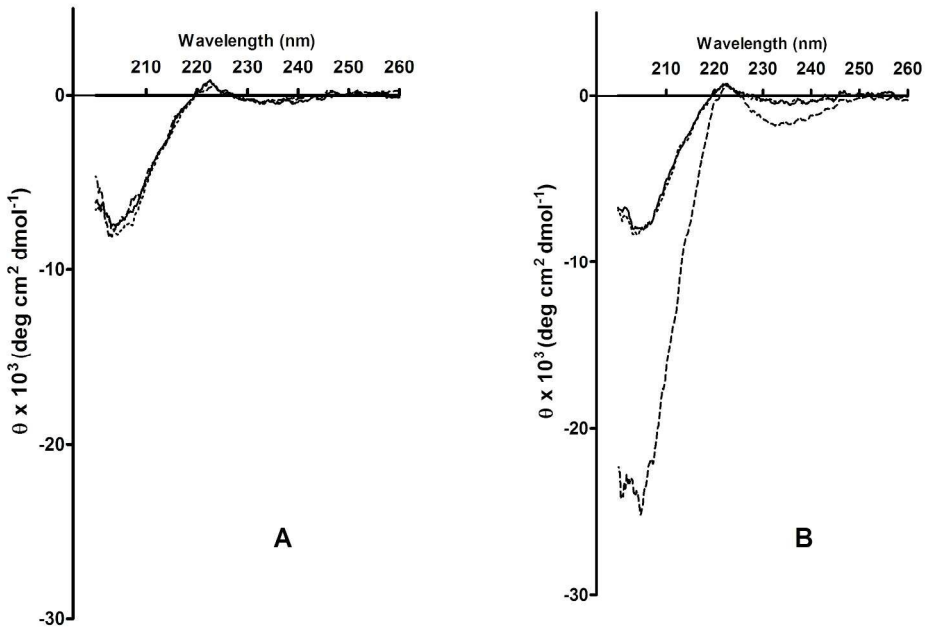

Figure 1:The effect of Cu(II) and Zn(II) ions on the CD signals of BK in water at neutral pH and different peptide concentrations. CD spectra of 35 μM (panel A) and 100 μM (panel B) of pure BK (solid lines) and in the presence of a twofold excess of Cu(II) (dashed lines) or Zn(II) (dotted lines) ions.
263x181mm (300 x 300 DPI)

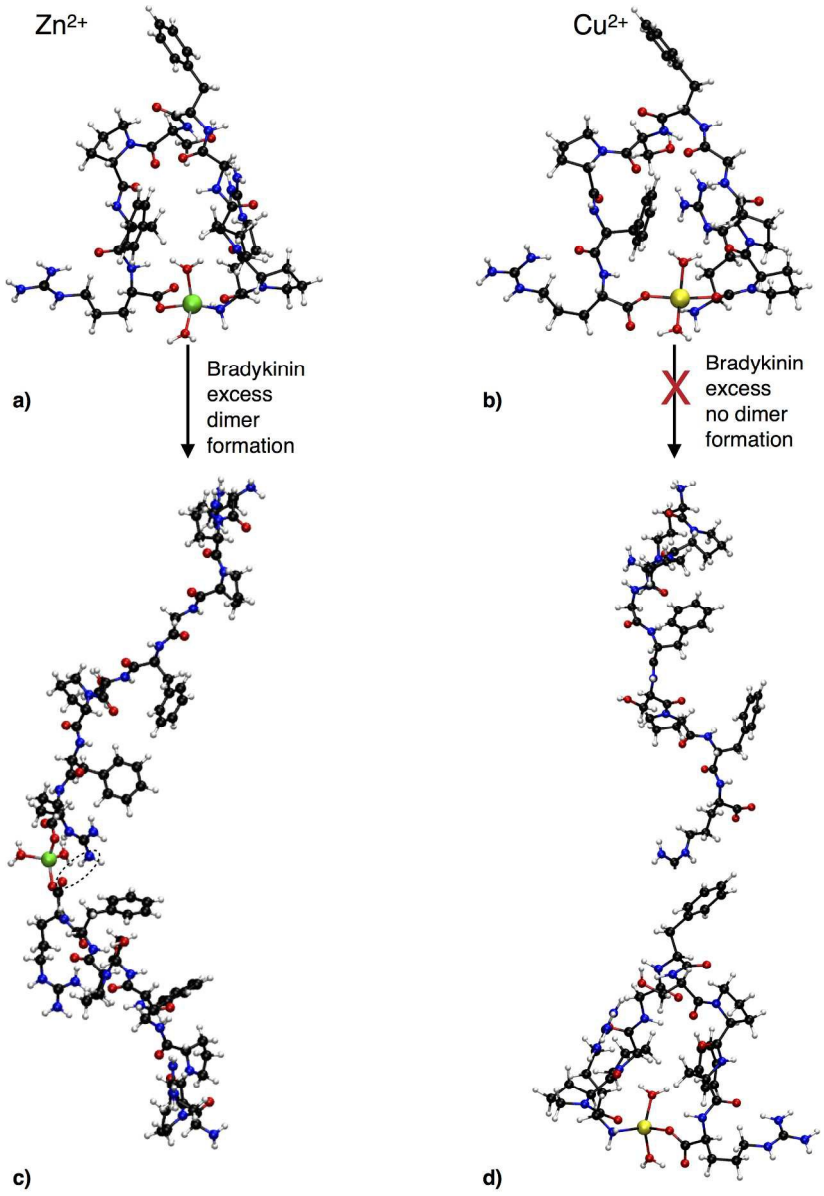

Figure 2: a) Coordination structure of Zn2+ complex with BK. b) Coordination structure of Cu2+ complex with BK. c) Coordination structure of the dimeric complex of Zn2+ with BK. The weak interaction between the C-terminal Arg and the carboxylic oxygen is circled. d) No dimer formation occurs with a 1:2 stoichiometric ratio of Cu2+ and BK.
201x281mm (300 x 300 DPI)

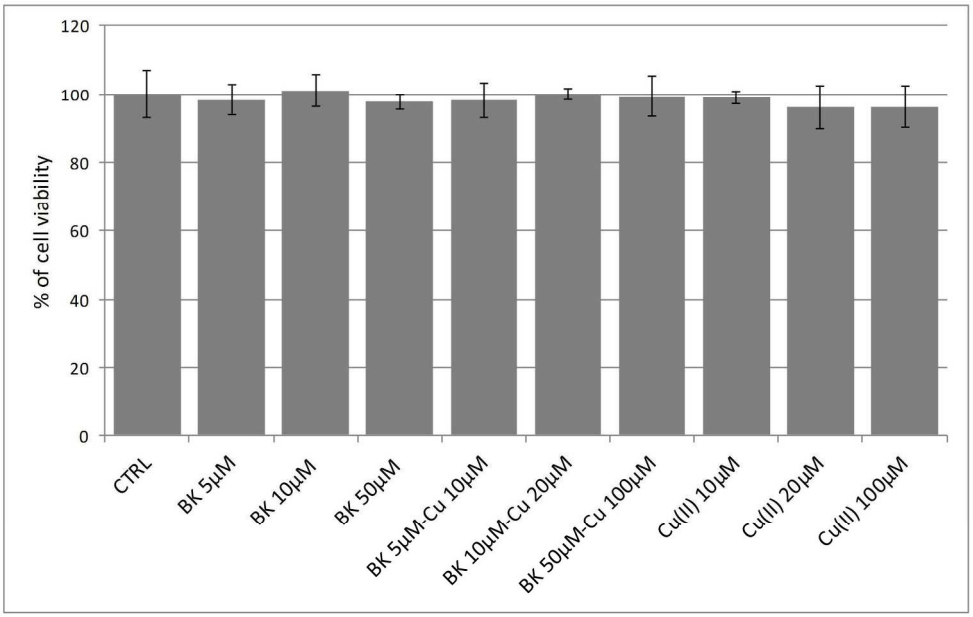

Figure 3: Dose response experiment to test the cell viability after treatment with BK, BK-Cu(II) and Cu(II). THP-1 cell cultures (undifferentiated monocytes) were incubated with increasing concentrations of BK and BK-Cu(II) for 20h and then cell viability was measured using MTT assay. Results are presented as the means ± SEM, the experiments were performed 3 times in triplicate.
189x121mm (300 x 300 DPI)

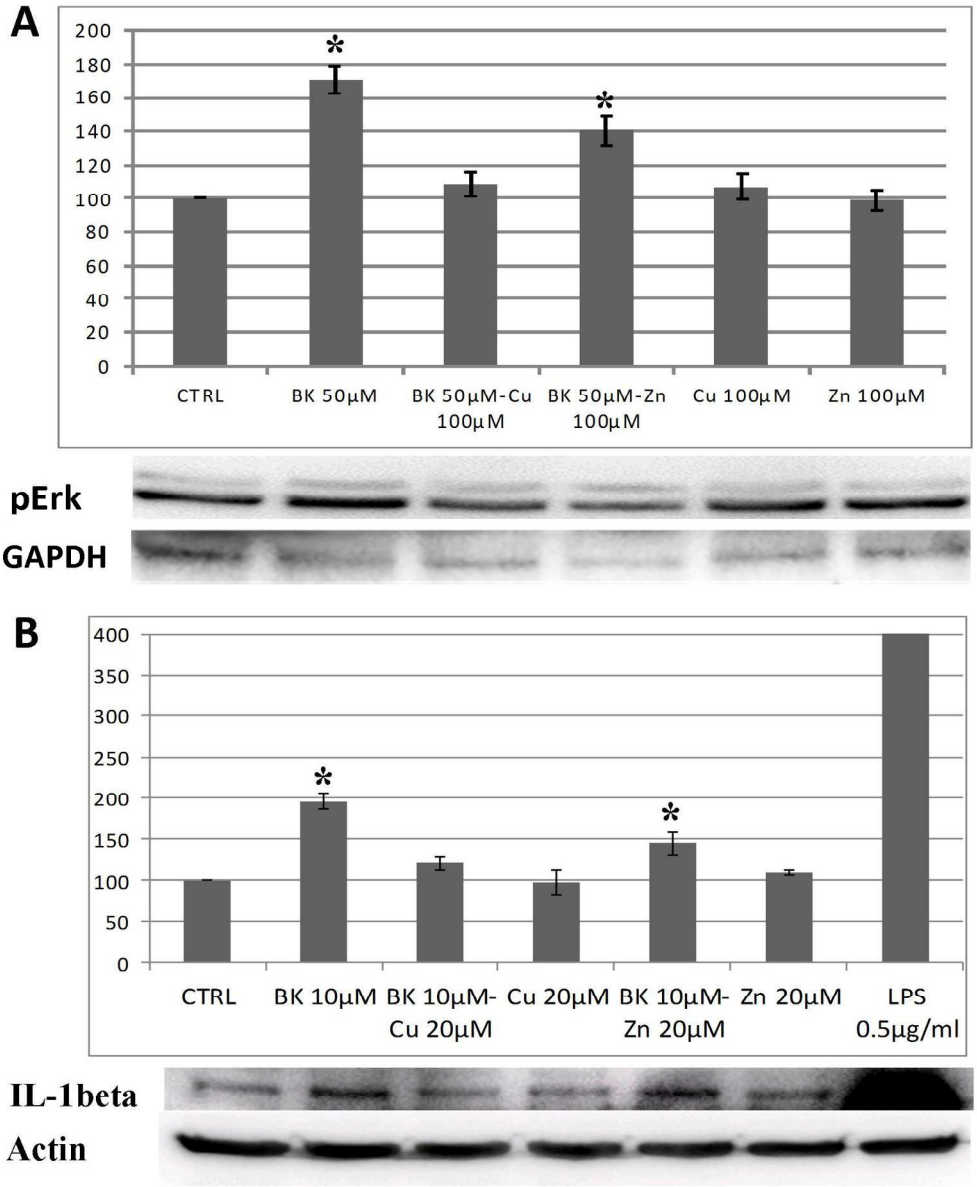

Figure 4:Expression of A) pErk1/2 and B) IL-1 beta in THP-1 cell cultures (undifferentiated monocytes) after 15 min and 20 hrs of treatment, respectively, with BK, copper or zinc alone, or BK pre-incubated with metals (1 h, ratio 1:2). Results are presented as mean ±SEM, the experiments were performed 3 times in triplicate. Asterisk (*) represents the correlation significant at the $p \leq 0.05$ level w.r.t. control, One-way Anova.
48869x58801mm (1 x 1 DPI)

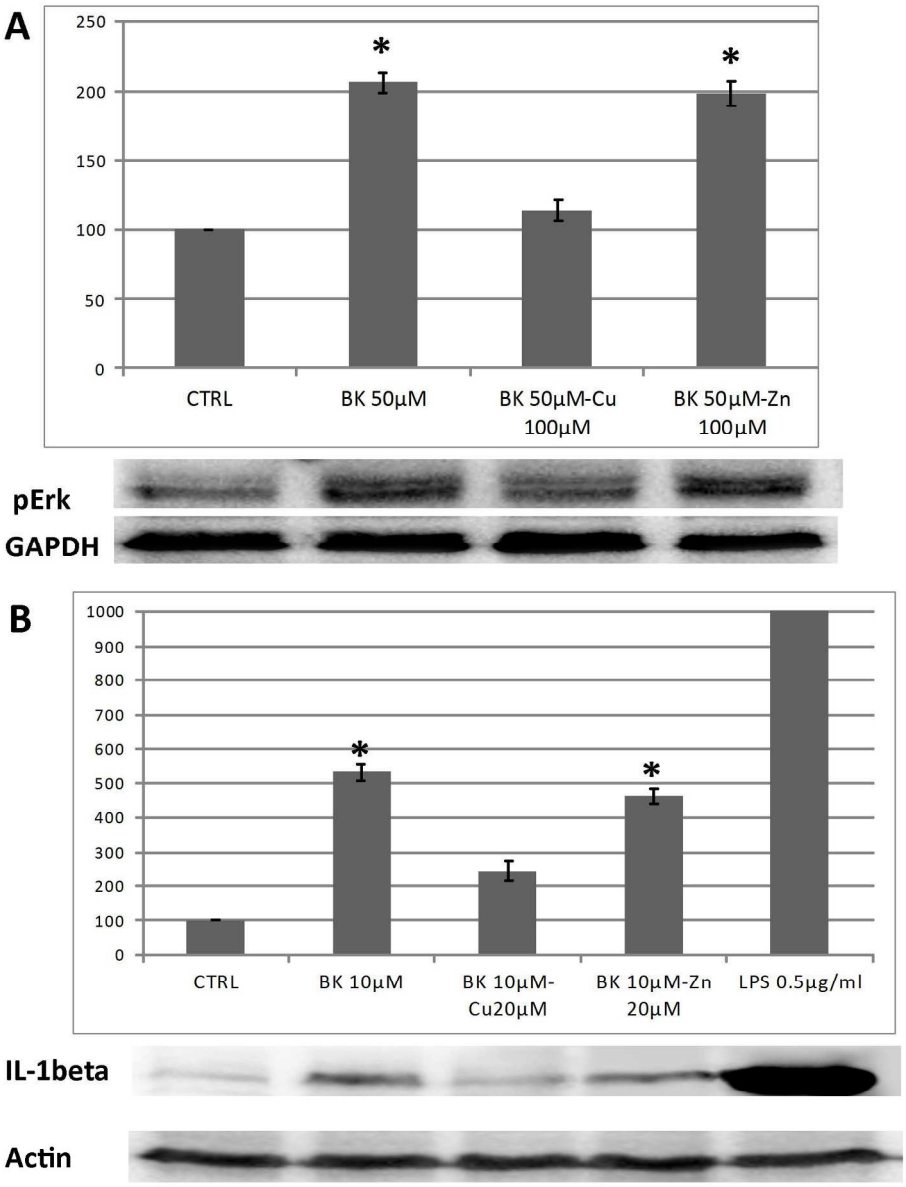

Figure 5: Expression of A) pErk1/2 and B) IL-1 beta in THP-1 cell cultures (differentiated monocytes: macrophages) after 15 min and 20 hrs of treatment, respectively, with BK or BK pre-incubated with copper or zinc (1 h, ratio 1:2). Results are presented as mean ±SEM, the experiments were performed 3 times in triplicate. Asterisk (*) represents the correlation significant at the $p \leq 0.05$ level w.r.t. control, One-way Anova.
50241x65531mm (1 x 1 DPI)

Bradykinin (BK) is recognized to be an inflammatory mediator and recent data also support an anti-inflammatory role of BK in Alzheimer's disease (AD). On the other hand, copper and zinc dyshomeostasis have been demonstrated to be largely involved with AD. In this scenario, it is important to understand how these metal ions interact with BK and if such interaction can affect BK activity. We report here that BK conformation and oligomerization status is strongly affected by copper but not zinc and this in turn affects BK activity in cells. The results obtained open to further role of metal ions, particularly copper, in the development and outcome of neuroinflammatory diseases.